THE JOURNAL OF BIOLOGICAL CHEMISTRY VOL. 285, NO. 14, pp. 10748–10760, April 2, 2010

Filamin B Plays a Key Role in Vascular Endothelial Growth Factor-induced Endothelial Cell Motility through Its Interaction with Rac-1 and Vav-2*[S]

Received for publication, September 7, 2009, and in revised form, January 25, 2010 Published, JBC Papers in Press, January 28, 2010, DOI 10.1074/jbc.M109.062984

Beatriz del Valle-Pérez[‡§], Vanesa Gabriela Martínez[§], Cristina Lacasa-Salavert[‡§], Agnès Figueras[§], Sandor S. Shapiro[¶†], Toshiro Takafuta[‖], Oriol Casanovas[§], Gabriel Capellà[§], Francesc Ventura[‡], and Francesc Viñals[‡§1]

From the [‡]Unitat de Bioquímica i Biologia Molecular, Departament de Ciències Fisiològiques II, Universitat de Barcelona-IDIBELL and the [§]Laboratori de Recerca Translacional, Institut Català d'Oncologia-IDIBELL, L'Hospitalet de Llobregat, E-08907 Barcelona, Spain, the [¶]Department of Molecular Physiolgy and Biophysics, Jefferson Medical College of Thomas Jefferson University, Philadelphia, Pennsylvania 19107, and [‖]Nishi-Kobe Medical Center, Kobe, Hyogo 651 2273, Japan

Actin-binding proteins filamin A (FLNA) and B (FLNB) are expressed in endothelial cells and play an essential role during vascular development. In order to investigate their role in adult endothelial cell function, we initially confirmed their expression pattern in different adult mouse tissues and cultured cell lines and found that FLNB expression is concentrated mainly in endothelial cells, whereas FLNA is more ubiquitously expressed. Functionally, small interfering RNA knockdown of endogenous FLNB in human umbilical vein endothelial cells inhibited vascular endothelial growth factor (VEGF)-induced *in vitro* angiogenesis by decreasing endothelial cell migration capacity, whereas FLNA ablation did not alter these parameters. Moreover, FLNB-depleted cells increased their substrate adhesion with more focal adhesions. The molecular mechanism underlying this effect implicates modulation of small GTP-binding protein Rac-1 localization and activity, with altered activation of its downstream effectors p21 protein Cdc42/Rac-activated kinase (PAK)-4/5/6 and its activating guanine nucleotide exchange factor Vav-2. Moreover, our results suggest the existence of a signaling complex, including FLNB, Rac-1, and Vav-2, under basal conditions that would further interact with VEGFR2 and integrin $\alpha v\beta 5$ after VEGF stimulation. In conclusion, our results reveal a crucial role for FLNB in endothelial cell migration and in the angiogenic process in adult endothelial cells.

Angiogenesis, or the formation of new blood vessels from preexisting vasculature, is an essential part of many physiological processes, including wound healing and the female menstrual cycle. However, stimulated blood vessel growth is also found in many disease states, such as tumor growth, diabetic retinopathy, and arthritis (1–3). Among the best studied inducers of angiogenesis are VEGF,[2] fibroblast growth factor 2, transforming growth factor-β, and angiopoietins.

Angiogenesis is a complex process with several stages, including disruption of the intercellular junctions, extracellular matrix remodeling, sprouting, endothelial cell proliferation, and migration. The alterations that allow this process are reversible because once at their destination, endothelial cells stop dividing, regenerate the extracellular matrix, and reestablish intercellular contacts (3–5). All of these changes require major reorganization of the endothelial cell cytoskeleton, the integrity of which is essential for the maintenance of cell structure. Furthermore, it is known that remodeling of the actin cytoskeleton accompanies alterations in cell shape and motility during processes such as normal organogenesis, oriented nerve and capillary growth, and angiogenesis (6). A host of actin-binding proteins play a role in cytoskeletal organization (6, 7), many of which are also involved in connecting the plasma membrane and its integral proteins, such as integrins, with the actin cytoskeleton (8). The actin-binding protein family includes talin, vinculin, α-actininin, and the filamins, among others. Endothelial cells contain high levels of these proteins, presumably in order to maintain a structured actin cytoskeleton and the capacity to respond to signals that will affect motility and cell structure. Factors that induce motility of endothelial cells, such as angiogenic cytokines (VEGF and fibroblast growth factor 2), affect the actin cytoskeleton and also actin-binding proteins (9–11).

Filamins bind actin through their N-terminal actin-binding domain (ABD), whereas the C-terminal 24th repeat is essential for filamin dimerization (12–14). The ABD is followed by a series of 24 repeated sequences of ~100 amino acids that func-

* This work was supported, in whole or in part, by National Institutes of Health Grant HL-072439 (to S. S. S. and T. T.). This work was also supported by Ministerio de Ciencia y Tecnología Grants SAF2004-01350, SAF2007-60955, and RTICC RD2006-0092 (to F. Viñals) and BFU2008-02010 to (F. Ventura), Generalitat de Catalunya Grants 2005SGR727 and 2009SGR283 (to F. Viñals), and a grant from the National Hemophilia Foundation, Delaware Valley Chapter (to S. S. S.).

This paper is dedicated to the memory of Dr. Sandor S. Shapiro, who passed on in July 2007 while experimental work was in progress.

[S] The on-line version of this article (available at http://www.jbc.org) contains supplemental Figs. S1–S4 and Videos 1 and 2.

[†] Deceased July 21, 2007.

[1] To whom correspondence should be addressed: Laboratori de Recerca Translacional, Institut Català d'Oncologia-IDIBELL, Gran Via S/N KM 2,7, E-08907 L'Hospitalet de Llobregat, Barcelona, Spain. Tel.: 34-93-260-7344; Fax: 34-93-260-7466; E-mail: fvinyals@ico.scs.es.

[2] The abbreviations used are: VEGF, vascular endothelial growth factor; HUVEC, human umbilical vein endothelial cell(s); FCS, fetal calf serum; GFP, green fluorescent protein; siRNA, small interfering RNA; PBS, phosphate-buffered saline; MAPK, mitogen-activated protein kinase; GST, glutathione *S*-transferase; GAP, GTPase-activating protein; FLNA and -B, filamin A and B, respectively.

tion as domains of protein-protein interaction; so far, more than 30 different proteins have been described as interacting with filamins. The function of filamins seems to be dual: first, helping to form a three-dimensional network of actin through their actin-binding domain; and second, acting as scaffolding proteins offering docking sites for cytoplasmic proteins, membrane receptors, integrins, etc. Thus, filamins connect plasma membrane with the intracellular cytoskeleton and are involved in changes in cell shape (12–14). Three filamins have been described: filamin A, or ABP280, is the most abundant and is widely expressed in different tissues; filamin B is also broadly expressed; and filamin C is mainly expressed in skeletal muscle (12–14). High levels of filamin A and filamin B have previously been detected in vessels (15–17) and in endothelial cells in culture (17–19). Knock-out experiments show the functional importance of each isoform: filamin A knock-out mice die during development due to aberrant vascular patterning and cardiac defects (20, 21), whereas filamin B deficiency in mice mainly causes skeletal malformations (22–24) and vascular deficiencies (23).

In order to study the role of both filamins A and B in vascular endothelial cells, we abrogated their expression in human umbilical vein endothelial cells (HUVEC) *in vitro*. Using this model, we show in this work a key role for filamin B in endothelial cell motility, exerted through its function as a scaffolding protein connecting VEGFR2, Vav-2, and Rac-1 proteins.

EXPERIMENTAL PROCEDURES

Materials

VEGF was from Calbiochem. Cell culture media, fetal bovine serum, glutamine, and antibiotics were obtained from Invitrogen or Biowhittaker. Other reagents were of analytical or molecular biology grade and were purchased from Sigma or Roche Applied Science.

Cell Culture and Transfections

Murine lung capillary endothelial cells (cell line 1G11) were obtained from Alberto Mantovani and Annunciata Vecchi (Instituto Ricerche Farmacologiche Mario Negri, Milan, Italy) (25). They were cultured in Dulbecco's modified Eagle's medium, containing 20% FCS, 50 units/ml penicillin, 50 μg/ml streptomycin sulfate, 25 μg/ml endothelial cell growth supplement (BD Biosciences), 100 μg/ml heparin (Sigma), 1% non-essential amino acids, and 2 mM sodium pyruvate.

HUVEC were obtained from Advancell (Barcelona, Spain) and were cultured in M199 (Biowhittaker) supplemented with 20% FCS, 50 units/ml penicillin, 50 μg/ml streptomycin sulfate, 25 μg/ml endothelial cell growth supplement, 100 μg/ml heparin, 2 mM sodium pyruvate, 1 mM HEPES, pH 7.4. HUVEC were transiently transfected using Lipofectamine 2000. Plasmids used were GFP, GFP-Rac-1-Valine12 (a constitutively active form of Rac-1), and GFP-Rac-1-M7 (a dominant negative form of Rac-1), the last two a generous gift from Dr. Alan Hall (Memorial Sloan-Kettering Cancer Center, New York).

Human siRNAs for FLNB and FLNA were constructed using the Silencer™ siRNA construction kit (Ambion), according to the manufacturer's instructions. Three independent sequences for human filamin B and two independent sequences for human filamin A were designed with free Whitehead Institute software (available on the World Wide Web). siRNA-FLNB1 corresponded to 5′-AAGCTCCCTTAAAGATATTTG-3′ (nucleotides 2031–2051 of filamin B); siRNA-FLNB2 corresponded to 5′-AAGGTCCTTCCCACATATGAT-3′ (nucleotides 4529–4549); and siRNA-FLNB3 corresponded to 5′-AACACCTGAAGGGTACAAAGT-3′ (corresponding to nucleotides 7299–7319). siRNA-FLNA1 corresponded to 5′-AAGATGTCCTGCATGGATAAC-3′ (nucleotides 4637–4389 of filamin A). siRNA-FLNA2 corresponded to 5′-AAGACCACCTACTTTGAGATC-3′ (nucleotides 1370–1392). No similar sequences (with more than 17 identical nucleotides) were found in BLAST. Irrelevant siRNA corresponded to the negative universal control RNA interference (Invitrogen). For siRNA experiments, HUVEC were seeded in 6-well plates. Four hours before transfection, medium was changed to Opti-MEM I without antibiotics and supplemented with 20% FCS. siRNAs were then transfected with Lipofectamine 2000. The total amount of siRNA (final concentration 62.5 nM) was diluted in Opti-MEM I; in a different tube, Lipofectamine 2000 was also diluted in Opti-MEM I. After a 5-min incubation at room temperature, the transfection reagent mix was added to the siRNA and was further incubated for 20 min at room temperature. Cells were incubated with the reaction mix for 4 h. At the end of the incubation, cells were washed twice with Opti-MEM I without antibiotics and supplemented with 10% FCS. Media were replaced with 2 ml of complete Medium 199.

Tubulogenesis Assays

For HUVEC, 2×10^5 cells were seeded in triplicate in a 24-well plate coated with 300 μl of rat tail type-I collagen (1.2 mg/ml) in Dulbecco's modified Eagle's medium and 20% FCS and allowed to attach for at least 2 h. Following this, cells were overlaid with an additional 300 μl of collagen. Once the collagen had polymerized, cells were fed with M199 medium, 1% FCS, 100 μg/ml heparin, 150 μg/ml endothelial cell growth supplement, and 40 ng/ml VEGF. Following completion of network formation (24 h), 3 images/well were captured on a Leica inverted phase-contrast microscope DMIRBE equipped with digital capture software, and tubulogenesis was measured using ImageJ software.

Migration Assays

Migration was measured using a Boyden chamber. Transwell inserts (8-μm pore size; Costar) were coated with fibronectin (25 μg/ml) overnight at 4 °C. Transwells were washed with phosphate-buffered saline (PBS) and blocked with PBS containing 5% bovine serum albumin for 3 h at 37 °C. Transwells were rinsed with PBS and dried for 3 h in a laminar flow cabin.

HUVEC were seeded into the transwell (200,000/well), and after 1 h at 37 °C, migration was stimulated by the addition of 20 ng/ml VEGF. After 16 h, transwells were washed, and cells were fixed with 3% paraformaldehyde for 30 min. After four washes with PBS, they were stained with 5 μg/ml propidium iodide for 5 min and rinsed four times with PBS, and the upper surface was wiped to remove the non-migrating cells. Images were captured on a Leica inverted immunofluorescence microscope, and the migrating cells were counted.

Western Blotting

Cells were washed twice in cold PBS and lysed for 15 min at 4 °C in Triton X-100 lysis buffer (50 mM Tris-HCl, 100 mM NaCl, 50 mM NaF, 5 mM EDTA, 40 mM β-glycerophosphate, 200 μM sodium orthovanadate, 100 μM phenylmethylsulfonyl fluoride, 1 μM pepstatin A, 1 μg/ml leupeptin, 4 μg/ml aprotinin, 1% Triton X-100, pH 7.5). Western blotting was performed as described (26). The blots were incubated with polyclonal rabbit anti-filamin B antibody (17), monoclonal anti-filamin A antibody (Chemicon), polyclonal anti-PARP antibody (Cell Signaling), monoclonal anti-VEGFR2 antibody (Santa Cruz Biotechnology, Inc., Santa Cruz, CA), polyclonal anti-VEGFR1 antibody (Santa Cruz Biotechnology, Inc.), monoclonal anti-RhoA antibody (Santa Cruz Biotechnology, Inc.), polyclonal anti-phospho-VEGFR2 (Tyr^{1175}; Cell Signaling), polyclonal anti-phospho-Src antibody (Tyr^{527}; Cell Signaling), polyclonal anti-Src (Cell Signaling), monoclonal anti-Rac-1 antibody (Upstate), polyclonal anti-phospho-PAK-4/5/6 antibody (Cell Signaling), polyclonal anti-PAK-4 antibody (Cell Signaling), polyclonal anti-phospho-Vav-2 antibody (Santa Cruz Biotechnology, Inc.), polyclonal anti-Vav-2 antibody (Santa Cruz Biotechnology, Inc.), monoclonal anti-phospho-ERK antibody (Sigma), polyclonal anti-ERK1/2 antibody (27), monoclonal anti-α-tubulin antibody (Sigma), or monoclonal anti-β-actin antibody (Sigma) in blocking solution overnight at 4 °C.

Immunoprecipitation

Quiescent HUVEC stimulated or not with 10 ng/ml VEGF for 5 min were lysed with octyl glucopyranoside buffer (100 mM octyl glucopyranoside, 2 mM $CaCl_2$, 2 mM $MgCl_2$, 40 mM β-glycerophosphate, 200 μM sodium orthovanadate, 100 μM phenylmethylsulfonyl fluoride, 1 μM pepstatin A, 1 μg/ml leupeptin, 4 μg/ml aprotinin in PBS, pH 7.5) for 15 min at 4 °C. Insoluble material was removed by centrifugation at 13,000 × *g* for 20 min at 4 °C. Protein lysates (750 μg) were precleared with 30 μl of protein A/protein G-Sepharose beads (Amersham Biosciences) for 2 h at 4 °C, centrifuged at 13,000 × *g* for 10 min at 4 °C, and incubated overnight with monoclonal anti-VEGFR2 antibody (Santa Cruz Biotechnology, Inc.), polyclonal anti-VEGFR1 antibody (Santa Cruz), monoclonal anti-Rac-1 antibody (Upstate), monoclonal anti-RhoA antibody (Santa Cruz), polyclonal anti-Vav-2 antibody (Santa Cruz), or monoclonal anti-αvβ5 (Merck Farma y Química, Barcelona, Spain). Samples were incubated with 30 μl of protein A/protein G-Sepharose beads (Amersham Biosciences) for an additional 4 h at 4 °C. Precipitates were washed four times with Triton X-100 lysis buffer (50 mM NaF, 40 mM β-glycerophosphate, 200 μM sodium orthovanadate, 100 μM phenylmethylsulfonyl fluoride, 1 μM pepstatin A, 1 μg/ml leupeptin, 4 μg/ml aprotinin, 0.1% Triton X-100 in PBS, pH 7.5). The final pellet was resuspended in 50 μl of Laemmli sample buffer (28), followed by protein separation on an SDS-7.5% polyacrylamide gel and Western blotting as described before using the appropriate antibodies.

GST-Rac-1 Pull-down Assay

Quiescent HUVEC stimulated or not with 10 ng/ml VEGF for 5 min were lysed with Triton X-100 lysis buffer (50 mM NaF, 40 mM β-glycerophosphate, 200 μM sodium orthovanadate, 100 μM phenylmethylsulfonyl fluoride, 1 μM pepstatin A, 1 μg/ml leupeptin, 4 μg/ml aprotinin, 0.1% Triton X-100 in PBS, pH 7.5) for 15 min at 4 °C. Insoluble material was removed by centrifugation at 13,000 × *g* for 20 min at 4 °C. Protein lysates (750 μg) were incubated with equal amounts of GST or GST-Rac-1 (a generous gift from Dr. Mireia Duñach, Universitat Autònoma de Barcelona) overnight at 4 °C. After this time, 15 μl of glutathione-Sepharose beads (Amersham Biosciences) were added for an additional 4 h at 4 °C. Beads were washed four times with Triton X-100 lysis buffer. The final pellet was resuspended in 30 μl of Laemmli sample buffer, followed by Western blotting as described before with a polyclonal rabbit anti-filamin B antibody or a monoclonal mouse anti-GST.

Rac G-LISA

For measuring Rac-1-GTP levels, HUVEC cells were serum-starved overnight. Rac-1-GTP was detected using the colorimetric G-LISA Rac-1/2/3 activation assay (Cytoskeleton, Denver, CO). Briefly, cells were lysed according to the manufacturer's protocol. Total protein was measured, appropriately diluted in binding buffer, and incubated on 96-well plates that contained a Rac-GTP-binding protein linked to the bottom of each well. The bound Rac-GTP is detected with a Rac-specific primary antibody and a horseradish peroxidase-conjugated secondary antibody. The signal produced by the horseradish peroxidase detection reagent is proportional to the amount of Rac-GTP and can be detected by measuring absorbance at 595 nm. Appropriate controls were carried out (positive control was Rac-1 control protein, and negative control was lysis buffer alone).

Northern Blotting

Total RNA from cells was extracted using the phenol/chloroform method, and Northern blotting using 20 μg of RNA was performed as described (26). Blots were hybridized to mouse filamin B cDNA, to a fragment of the 3′-end of the human filamin A sequence (a generous gift from Dr. Saret (National Institutes of Health)) or to rat glyceraldehyde-3-phosphate dehydrogenase cDNA labeled with [α-^{32}P]dCTP (Amersham Biosciences).

Immunofluorescence Studies

Two-dimensional Cell Immunofluorescence—Cells were cultured on glass coverslips for 24 h, rinsed three times with PBS, and fixed in 3% paraformaldehyde for 30 min. After four washes with PBS, they were permeabilized with PBS, 0.2% Triton X-100 for 5 min, rinsed four times with PBS and blocked for 30 min at room temperature in PBS containing 2% bovine serum albumin. Coverslips were incubated with polyclonal rabbit anti-filamin B antibody (17), monoclonal anti-filamin A antibody (Chemicon), monoclonal anti-Rac-1 antibody (Upstate), or monoclonal anti-vinculin antibody (Sigma), followed by 5 μg/ml Alexa 488 anti-rabbit or Alexa 568 anti-mouse (Molecular Probes) for 1 h at room temperature. To visualize F-actin, coverslips were incubated with red-phalloidin or 633-phalloidin (colored blue) 1 μg/ml (Sigma) for 1 h. Coverslips were mounted using Gel Mount (Biomedia), and fluorescence was

viewed with a Leica confocal microscope (LEICA spectral confocal TCS-SL, Serveis Científico Tècnics de la Universitat de Barcelona).

Tissue Immunofluorescence—Cryopreserved sections of mouse tissue were analyzed for filamin B (polyclonal rabbit antibody) (17), filamin A (monoclonal mouse antibody, Chemicon), PECAM/CD31 (monoclonal rat antibody, BD Pharmingen), von Willebrand factor (polyclonal rabbit antibody, Dako), and α-smooth muscle actin (polyclonal rabbit antibody, LabVision). Primary antibodies were incubated overnight at 4 °C (1:50). Nuclei were stained with TO-PRO-3 iodide 642/661 (0.2 μM; Molecular Probes). Appropriate secondary antibodies bound to the appropriate fluorochrome (Molecular Probes) were used. Negative controls (lacking primary antibody but containing the secondary antibody) confirmed the specificity of the staining.

Tissue Immunohistochemistry—Sections from representative paraffin blocks of mouse tissues were deparaffined, rehydrated, and blocked for endogenous peroxidase activity using 3% H_2O_2. Antigen was retrieved with heat in sodium citrate buffer (8.2 mM trisodium citrate dihydrate and 1.98 mM citric acid, pH 6.0) or digestion with 0.1% trypsin in 1× PBS buffer. Primary polyclonal rabbit anti-filamin B antibody (1:10) was incubated for 16 h. Appropriate secondary antibodies were used. After development with diaminobenzidine, substrate was counterstained with Harris's hematoxylin. No staining was observed with negative control samples (absence of primary antibody or incubation with an irrelevant antibody or IgG).

Time Lapse Imaging

After transfection with siRNAs and GFP (to visualize transfected cells), HUVEC were starved for 12 h and then cultured for a further 12 h in the presence of 20 ng/ml VEGF. During these 12 h, GFP-positive cells were imaged by phase-contrast every 5 min on a LEICA spectral confocal TCS-SL with a ×20 objective. Images were analyzed using ImageJ software. We performed analysis of the track of 10 different cells from two independent experiments.

Cell Cycle Analysis

After transfection with siRNAs, HUVEC were starved for 12 h and then cultured for a further 12 h in basal medium or complete medium. Cells were then trypsinized and pooled with floating cells in the culture medium, washed, and fixed in 70% ethanol in PBS; they were kept in ethanol at −20 °C for at least 24 h. For staining, cells were washed to remove ethanol and resuspended in PBS with 100 μg/ml RNase and 40 μg/ml propidium iodide and then incubated at 37 °C for at least 30 min before flow cytometry analysis.

Statistical Analyses

Statistical significance of differences between the effects of unrelated siRNA and siRNAs against filamins were determined using Student's *t* test. In all experiments, differences were considered statistically significant when p was <0.05.

RESULTS

To confirm the vascular expression of filamins A and B, we performed immunofluorescence and immunohistochemistry on sections of adult mouse tissues (lung, kidney, adipose tissue, and testis). Using immunofluorescence on cryopreserved tissue sections, we detected low filamin B expression in parenchymal cells of lung (data not shown) and testis (supplemental Fig. S1*A*) and high expression levels in blood vessels, with a pattern very similar to that of PECAM/CD31, a classical endothelial cell marker. In contrast, we found high expression of filamin A in the parenchyma and in the different cell types that form the vessels, endothelial and mural cells, co-localizing with von Willebrand factor (a marker of endothelial cells) and with α-smooth muscle actin (a mural cell marker) (supplemental Fig. S1*A*). Both types of filamins, A and B, were expressed in endothelial cells. Using immunohistochemistry, we detected filamin B expression in vessels of lung, kidney, and adipose tissue (supplemental Fig. S1*B*), with lower levels observed in parenchymal cells. Taken together, these results indicate that the expression pattern of filamins in vessels is isoform-specific, with filamin A expressed at similar levels in the different cell types, whereas filamin B expression was concentrated mainly in endothelial cells.

Next, we analyzed filamin A and B expression in different cell lines and primary cultures by performing Northern blotting experiments using specific probes for filamin A and B and Western blotting experiments using specific antibodies. Using these reagents, we detected high levels of filamin B (both mRNA and protein) in primary HUVEC cultures (Fig. 1, *A* and *B*) and other endothelial cell lines, such as 1G11 (a murine lung capillary endothelial cell line) (25) and H5V (a mouse heart endothelial cell line transformed by polyoma middle T antigen) (29) (supplemental Fig. S1*C*) compared with other cell lines. We also detected filamin B protein expression in HeLa, C2C12, and HT29 (human colorectal adenocarcinoma) cells, but expression levels in these cell lines were much lower than those of endothelial cells (Fig. 1, *A* and *B*, and supplemental Fig. S1*C*). In contrast, filamin A was expressed at roughly the same levels in the different cell types studied, including endothelial cells (Fig. 1, *A* and *B*), further confirming the high levels of endothelial FLNB expression and a broader expression of FLNA in various cell types.

In order to study the role of filamin A and B in vascular endothelial cells, we chose primary cultures of HUVEC because they are much more representative of normal endothelial cell physiology as compared with the other cell lines. We sought to elucidate the functional importance of each filamin isoform in HUVEC tubule formation by an *in vitro* angiogenesis assay. To do so, we generated three independent siRNAs against three different sequences of human filamin B mRNA (siRNA-FLNB1, -2, and -3) and two siRNAs for filamin A (siRNA-FLNA1 and -2). We transfected HUVEC with these siRNAs and evaluated their effects on filamin A and filamin B expression by Western blotting. We found that siRNA-FLNB1 decreased filamin B expression by 40–60%, whereas siRNA-FLNB2 and siRNA-FLNB3 were the most effective with a decrease in filamin B levels of 70–80%; these siRNAs showed no effect on filamin A expression (Fig. 1*C*). The siRNAs against filamin A caused a dramatic decrease in filamin A protein levels, an effect that appeared to be compensated by an increase in filamin B expression (Fig. 1*C*). To evaluate the role of filamins in *in vitro* angio-

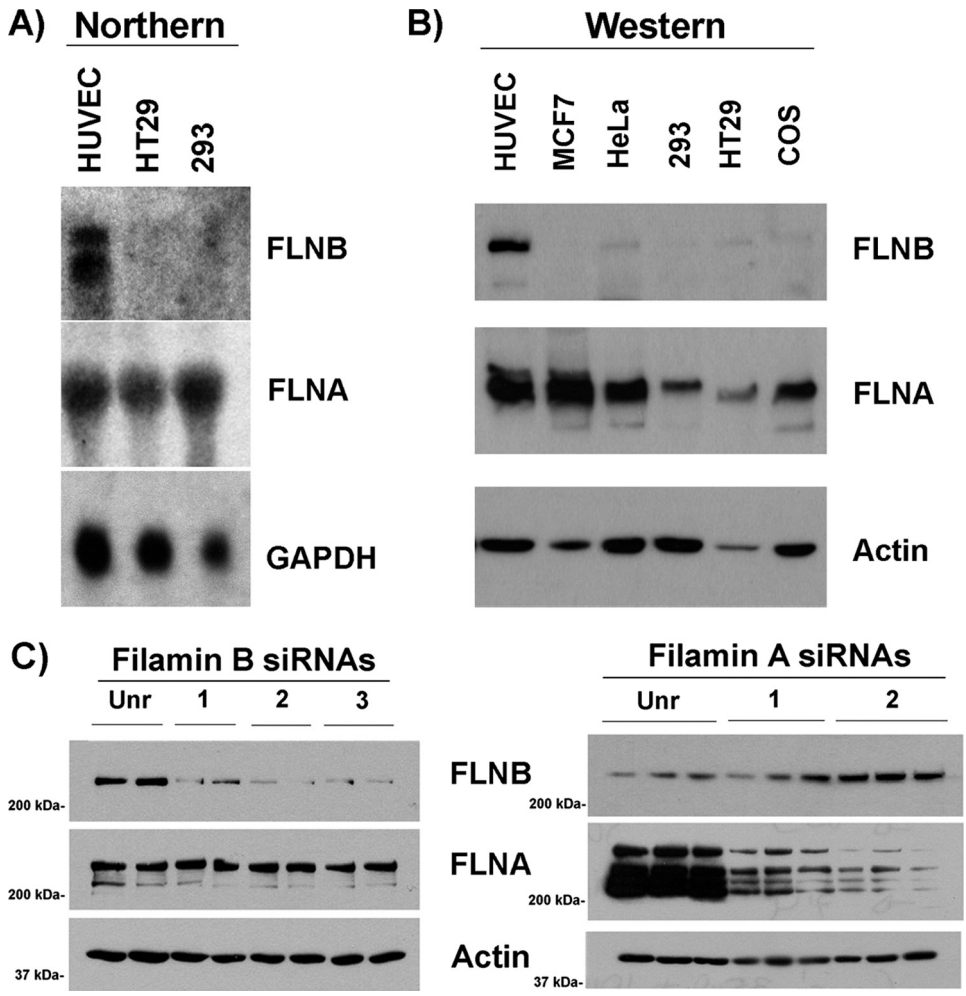

FIGURE 1. **Filamin A- and B-specific knockdown by siRNA transfection in endothelial cells.** *A*, Northern blotting analysis. HUVEC, HT29, and HEK-293 (human embryonic kidney) cells are shown. Filamin B, filamin A, and glyceraldehyde-3-phosphate dehydrogenase (as a loading control) were detected using specific probes. A representative Northern blot of three different experiments is shown. *B*, Western blotting analysis. HUVEC, MCF7 (human breast cancer), HeLa (human cervical adenocarcinoma), HEK-293, HT29, and COS (green monkey kidney) cells are shown. Filamin B, filamin A, and actin (as a loading control) were analyzed by immunoblotting. A representative blot of three different experiments is shown. *C*, HUVEC were transiently transfected with a control unrelated siRNA (*Unr*), siRNA-FLNB1 (*1*), siRNA-FLNB2 (*2*), siRNA-FLNB3 (*3*), siRNA-FLNA1 (*1*), or siRNA-FLNA2 (*2*), as described under "Experimental Procedures." After 48 h, cells were lysed as described, and filamin B (FLNB), filamin A (FLNA), or β-actin (as a loading control) were detected by immunoblotting. Two (for siRNA-FLNB) or three (for siRNA-FLNA) independent experiments are shown for each siRNA.

genesis, we transfected HUVEC with these siRNAs and, 24 h later, cultured the cells for an additional 24 h in type-I collagen gels in the absence or presence of the most important proangiogenic factor, VEGF (Fig. 2*A*). When cells were analyzed for their capacity to form tubular structures in type-I collagen gels, we discovered that siRNA-FLNBs blocked VEGF-induced tubulogenesis. In contrast, when we evaluated the effect of the siRNAs designed against filamin A on *in vitro* angiogenesis in collagen gels, we found that they did not affect endothelial cell reorganization after VEGF treatment (Fig. 2*A*).

Next, we searched for a mode of action for filamin B that could explain the results obtained in the *in vitro* assay. Transfection of HUVEC with the different siRNAs did not affect endothelial cell apoptosis or proliferation (supplemental Fig. S2, *A* and *B*). This effect was also confirmed by the lack of effect of filamin B depletion on a typical proliferation signaling pathway (ERK stimulation; see Fig. 5*B*). We next studied a possible role for this protein in endothelial cell migration. Given the role of filamins as actin-binding proteins, we hypothesized that filamin B could influence this process. Thus, we measured migration in Boyden chambers of HUVEC transfected with control, filamin A, or filamin B siRNAs and stimulated or not with VEGF. As observed in Fig. 2*B*, ablation of filamin B decreased basal HUVEC migration (55 and 78% decrease for siRNA-FLNB2 and -FLNB3, respectively) and abolished VEGF-stimulated cell migration. However, down-regulation of filamin A caused only a 22% decrease in basal migration and did not affect VEGF-stimulated migration. These data confirm the critical role of filamin B in endothelial cell migration and, consequently, in angiogenesis, whereas filamin A appears to play a secondary and less important role in this process.

In order to identify the mechanisms through which filamin B affects cell migration, we first evaluated the effect of VEGF stimulation on cytoskeletal organization in control or filamin B-depleted HUVEC. Cells depleted of filamin B presented a flat aspect and a larger size as compared with control cells (Fig. 3*A*). After VEGF stimulation, control and filamin B-depleted cells increased stress fiber formation. However, cells with low levels of filamin B presented multiple cellular protrusions with polymerized F-actin in different directions (Fig. 3*A*). In order to confirm these results, we performed time lapse microscopy. Cells were treated with VEGF and left to migrate; images were then captured for the following 12 h. We compared the random migration of HUVEC treated with siRNA-FLNB or control siRNA. Using this approach, we observed that control cells presented a normal migration pattern, defining a migration front and retracting the rear of the cell in order to advance (supplemental Video 1). In contrast, filamin B ablation decreased the track and speed of migration (33.8 ± 7.3 μm in 12 h in control cells, 15.6 ± 4.6 μm in 12 h in filamin B-depleted cells; $p < 0.001$), and, according to the previous results, cells presented different migration fronts and could not advance properly due to problems in retraction. Many cells ended up generating multiple protrusions in different directions (supplemental Video 2).

Our results so far suggested decreased migration of endothelial cells due to defects in the establishment of new adhesions or

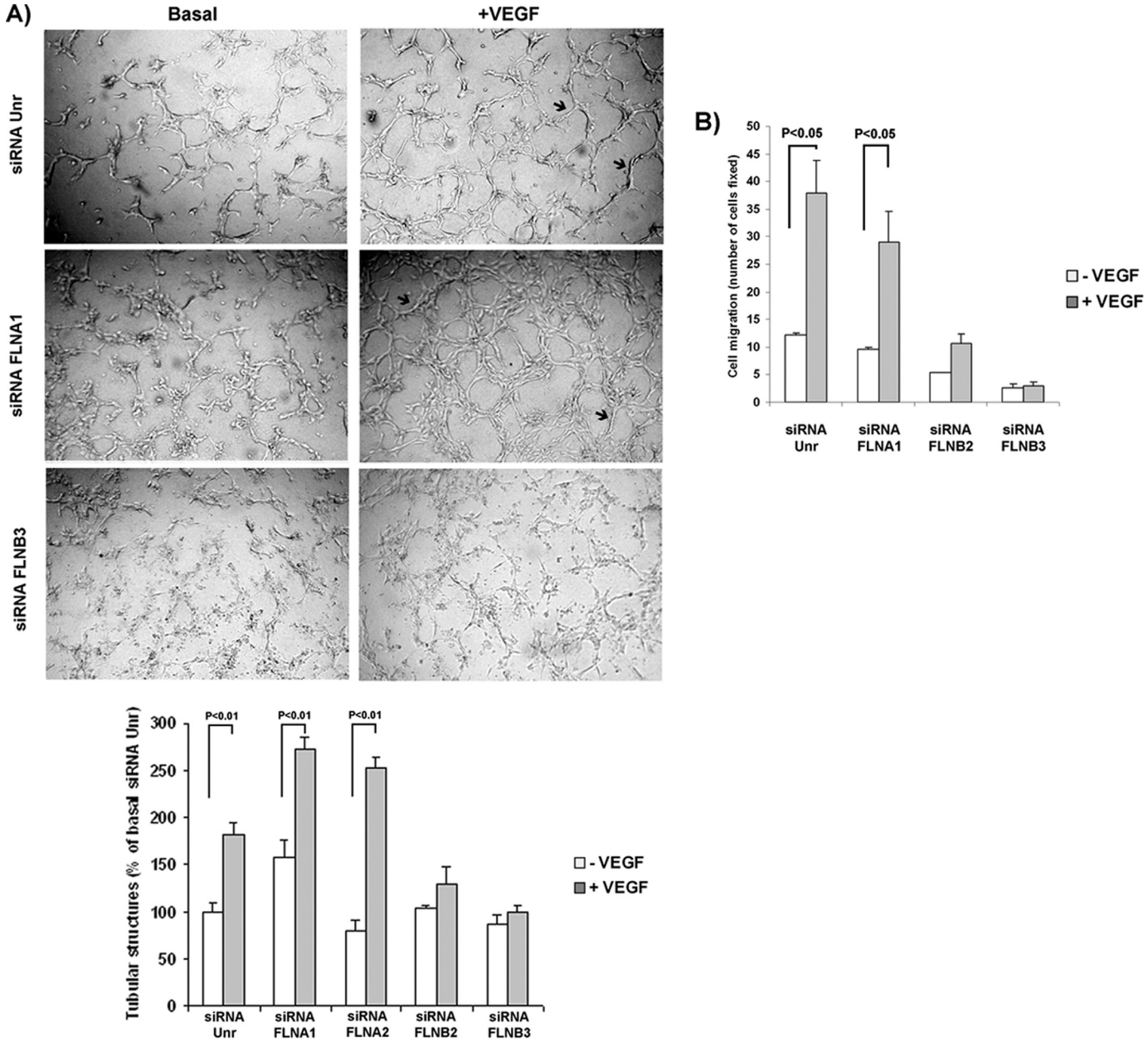

FIGURE 2. **Filamin B is essential for VEGF-induced *in vitro* angiogenesis and endothelial cell migration.** *A*, HUVEC were transiently transfected with an unrelated control siRNA, siRNA-FLNA1 and -FLNA2, or siRNA-FLNB2 and -FLNB3, as described. After 24 h, cells were trypsinized and immersed in collagen gels in the presence (+*VEGF*) or absence (*Basal*) of 40 ng/ml VEGF for an additional 24 h. Four independent images of each experiment were captured on a Leica inverted phase-contrast microscope (×10) to evaluate the tubule formation using ImageJ software (measurement of cell occupied surface). Results are the mean ± S.E. from three independent experiments. VEGF significantly stimulated tubular structures in control unrelated siRNA (*Unr*)- and in siRNA-FLNA1- and siRNA-FLNA2-treated cells (see *arrows*, $p < 0.01$, *t* test) without a significant effect on siRNA-FLNB2 and -FLNB3 cells. *B*, after transfection with the different siRNAs, cells were seeded into a Boyden chamber and left to migrate in the presence or absence of 20 ng/ml VEGF for 16 h. The number of migrating cells in basal conditions or after VEGF treatment was counted for every siRNA. We show the mean ± S.E. from three independent experiments. VEGF significantly stimulated cell migration in control unrelated siRNA- and in siRNA-FLNA-treated cells ($p < 0.05$, *t* test) without a significant effect on cells transfected with siRNA-FLNB2 or -3. siRNA-FLNA1, -B2, and -B3 caused a significant reduction in basal cell migration ($p < 0.005$, *t* test).

in retraction. To evaluate the effect of filamin B on adhesion to the extracellular matrix, we performed vinculin immunostaining using a specific antibody. As is shown in Fig. 3*B*, control HUVEC presented low levels of focal adhesions and contacts in the basal state, which increased after VEGF stimulation. Filamin B ablation caused a dramatic increase in focal adhesions and contacts in the basal state; the number of focal adhesions did not experience a further increase after VEGF stimulation. In contrast, siRNA-mediated filamin A knockdown did not affect the formation of adhesion contacts in basal or VEGF-stimulated conditions.

Different signaling pathways are activated by VEGF in order to stimulate endothelial cell migration. Focal adhesion kinase, its substrate paxillin, and the Rho family of GTPases are involved in focal adhesion turnover and stress fiber formation (10, 30, 31); phosphatidylinositol 3-kinase, ROCK (Rho-associated coiled-coil-containing protein kinase), p38 MAPK, MAPKAPK-2, and LIMK (LIM domain kinase 1) are involved in actin

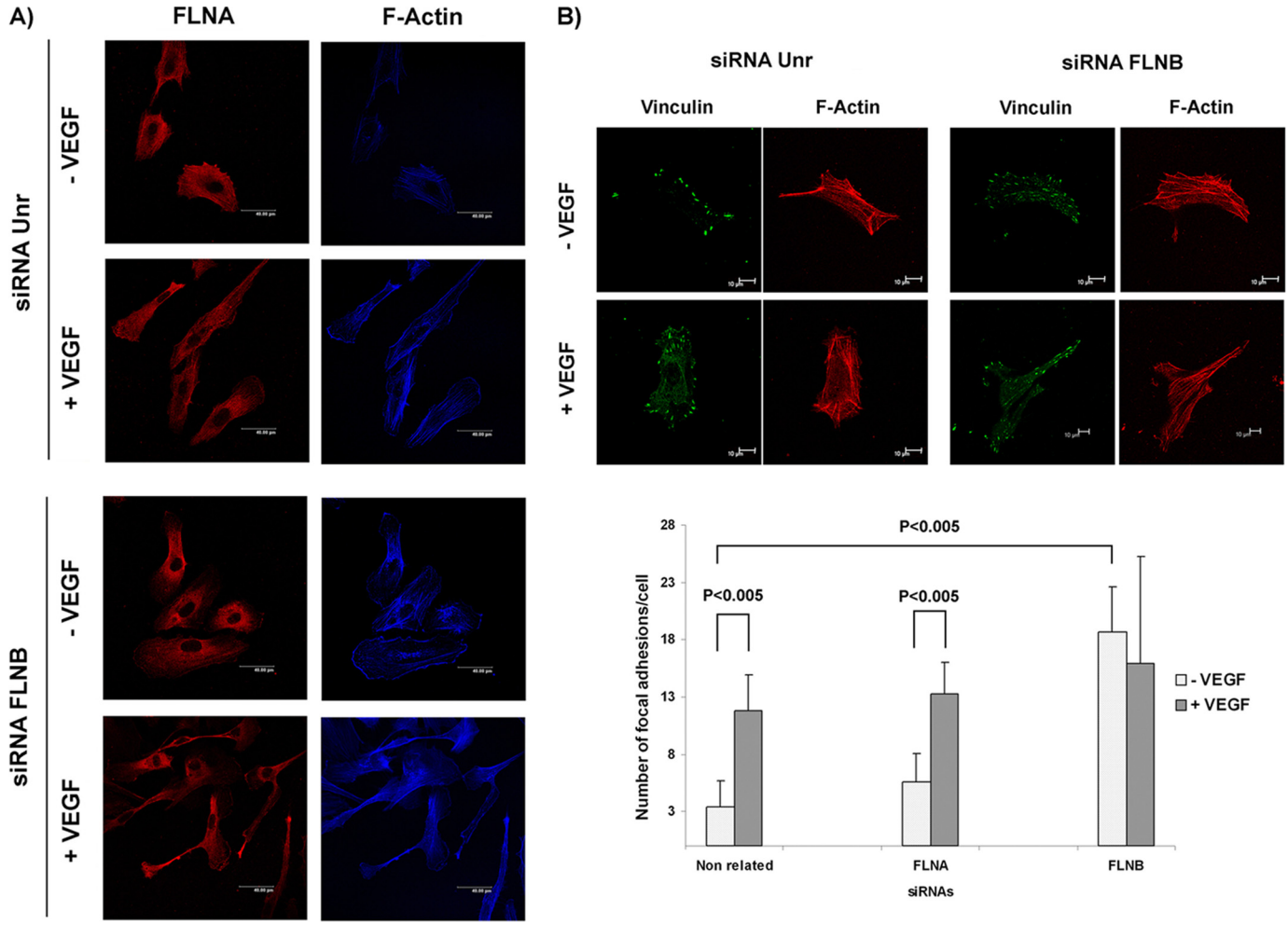

FIGURE 3. **Filamin B knockdown leads to an increase in focal adhesions.** *A*, immunolocalization of F-actin (*blue*) and filamin A (*red*) in HUVEC transiently transfected with an unrelated control siRNA (*Unr*) or siRNA-FLNB3 as described, in the absence (−*VEGF*) or presence of 20 ng/ml of VEGF for 30 min (+*VEGF*). *Bar*, 40 μm. *B*, immunolocalization of vinculin (*green*) and F-actin (*red*) in HUVEC transfected with an unrelated control siRNA and siRNA-FLNB3, in the absence or presence of 20 ng/ml VEGF for 30 min. *Bar*, 10 μm. The *graph* shows the quantification of focal adhesions in five independent experiments. VEGF significantly stimulated focal adhesions in control unrelated siRNA- and in siRNA-FLNA1-treated cells but not in siRNA-FLNB3 ($p < 0.005$, *t* test). siRNA-FLNB3 treatment significantly stimulated focal adhesions compared with basal levels ($p < 0.005$, *t* test).

reorganization (10, 32, 33); and Src kinases and integrins are involved in adhesion and extracellular matrix interaction (34, 35). As described previously, filamins interact with a large number of intracellular signaling proteins, membrane receptors, integrins, etc. that affect different intracellular signaling pathways. Taking into account the effects of our siRNAs in cell migration and shape, we hypothesized that filamin B could affect VEGF signaling through interaction with VEGF receptors, integrins, and the Rho family of small GTPase proteins, so we performed immunoprecipitation experiments using antibodies against Rac-1, RhoA, VEGF receptors (VEGFR1 and VEGFR2), and $\alpha v\beta 5$, an integrin that participates in angiogenesis. After immunoprecipitation, we detected filamin B by Western blotting. In basal conditions, we only detected interaction of filamin B with Rac-1 (Fig. 4*A*). After VEGF stimulation, filamin B not only maintained its interaction with Rac-1 but also coprecipitated with VEGFR2 and integrin $\alpha v\beta 5$ (Fig. 4*A*). In contrast, filamin B did not interact with RhoA or VEGFR1 (supplemental Fig. S3). In order to confirm these data, we performed pull-down assays using recombinant glutathione *S*-transferase (GST) fused to Rac-1. This construct but not GST specifically interacted with endogenous filamin B from basal or VEGF-stimulated HUVEC (Fig. 4*B*).

Next, we analyzed stimulation by VEGF of some of the migration signaling pathways in HUVEC cultures. In agreement with previous findings, we found stimulation of Rac-1 after 1 min of VEGF treatment and a later activation of PAK-4/5/6 (5 min) (supplemental Fig. S4). In contrast, we did not detect stimulation of LIMK or p38 MAPK at the times analyzed (data not shown). Taking into account these results and the observed interaction between filamin B and Rac-1, we analyzed the effect of filamin B depletion on the activity of Rac-1. Transfection of HUVEC with siRNAs against filamin B increased basal Rac-1 activity compared with cells transfected with an unrelated siRNA (Fig. 5*A*). Consistent with this increase in basal Rac-1 activity, activation of the Rac-1 substrate PAK-4/5/6 was also increased (Fig. 5*B*), even in the absence of VEGF, with a sustained stimulation of these proteins observed after VEGF addition. In contrast, analysis of VEGF-induced ERK activation in FLNB-depleted cells showed that the decrease in filamin B levels did not affect the capacity of VEGF to stimulate

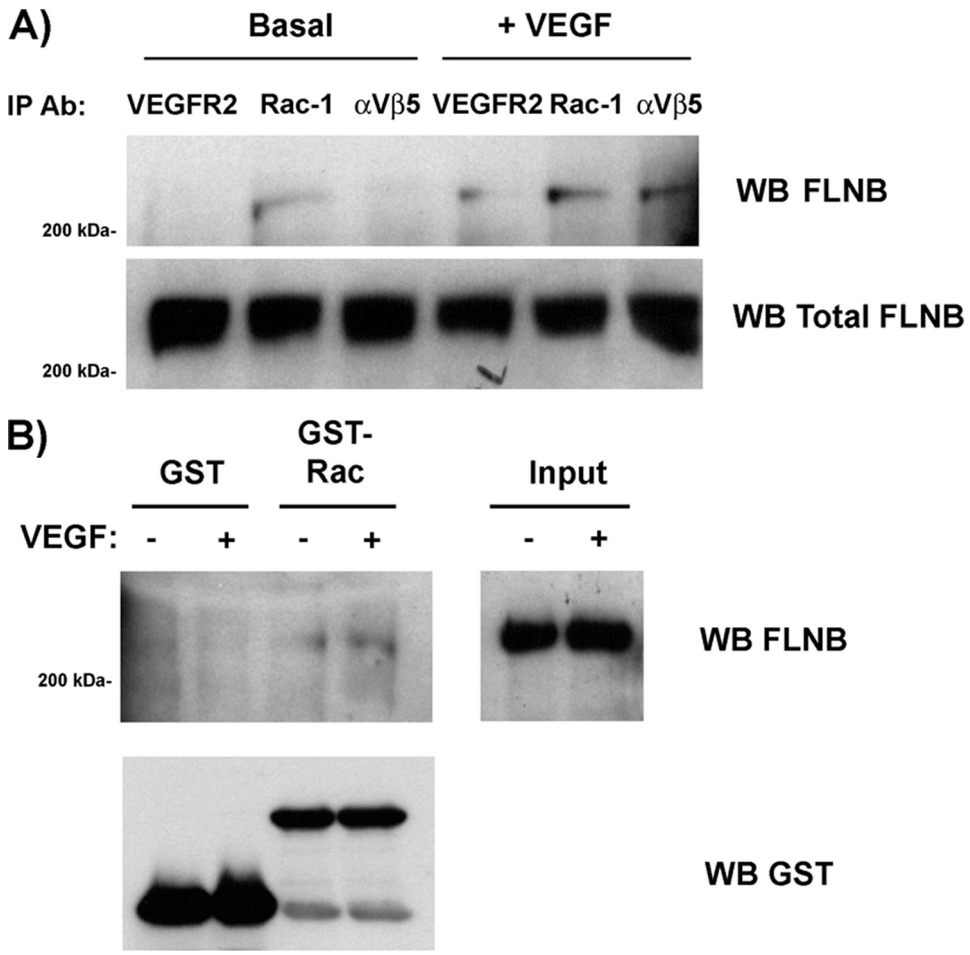

FIGURE 4. **Filamin B interacts with Rac-1 in basal conditions and with Rac-1, VEGFR2, and integrin $\alpha v\beta 5$ in VEGF-stimulated cells.** *A*, cells in basal conditions (*Basal*) or stimulated with 20 ng/ml VEGF for 5 min (+*VEGF*) were lysed, and VEGFR2, Rac-1, or $\alpha v\beta 5$ was immunoprecipitated (*IP*) with specific antibodies (*Ab*). Western blotting (*WB*) for filamin B was performed as described. As a loading control, Western blotting with total lysates before immunoprecipitation was also performed (total filamin B). A representative blot of three different experiments is shown. *B*, pull-down assay using GST or GST-Rac-1 recombinant proteins and lysates from cells in basal conditions (−) or stimulated for 5 min with 20 ng/ml VEGF (+). After pull down, Western blotting for filamin B or GST was performed as described before. A representative blot of two different experiments is shown.

ERK, which ruled out a nonspecific effect of filamin B depletion on general VEGF signal transduction (Fig. 5*B*).

Taking into account these results, we then evaluated whether filamin B depletion could affect normal Rac-1 function after VEGF stimulation. We first confirmed that ablation of filamin B by siRNA treatment did not modify Rac-1 total levels present in HUVEC (Fig. 6*A*). Next, we examined the effect of filamin B on Rac-1 subcellular location. As previously described, after VEGF stimulation of HUVEC, Rac-1 translocated to actin-rich membrane structures in the migration front (Fig. 6*B*). This translocation is essential for Rac-1 function (36–38). In contrast, when filamin B expression was decreased by siRNA treatment, Rac-1 accumulated in the intracellular compartment and was absent from the migration front (Fig. 6*B*). These data indicate that filamin B not only can affect Rac-1 activity but also can affect its intracellular location. Taken together, these results indicate that loss of filamin B altered normal Rac-1 cycles of activation/inactivation necessary for normal endothelial cell migration.

In order to address the importance of Rac-modulated effects in *in vitro* tubulogenesis, we overexpressed two different mutant variants of Rac-1: a constitutively active form (GFP-Rac-1-Valine12) and a dominant negative form of Rac-1 (GFP-Rac-1-M7). Increased activity of Rac-1 by overexpression of the Rac-1-V12 isoform resulted in HUVEC acquiring a flat phenotype (Fig. 7*A*), very similar to the one we observed following filamin B depletion. When we overexpressed the dominant negative form of Rac-1, we obtained a mixed effect, with some cells presenting a flat phenotype and others appearing unaffected (Fig. 7*A*). When we assayed cells transfected with each isoform in an angiogenesis assay *in vitro*, we found that transfection of either isoform caused cells to fail to be incorporated into pseudotubules (Fig. 7*B*), reinforcing the idea that a delicate control of Rac-1 activity is necessary for correct tubulogenesis.

We next studied whether filamin B could also affect other proteins involved in the Rac-1 signaling pathway. Rac-1 stimulation by VEGF is mediated by the guanine nucleotide exchange factor Vav-2 (39), which is in turn activated by phosphorylated Src. Much as happened with Rac-1, we demonstrated an interaction of filamin B (but not filamin A) and Vav-2 both in basal conditions and after VEGF stimulation (Fig. 8*A*). Taking into account that Rac-1 is overstimulated as a result of filamin B depletion, we speculated that filamin B siRNA treatment could also cause Vav-2 overstimulation. Surprisingly, we found that in contrast with our previous observations, filamin B depletion abolished Vav-2 stimulation by VEGF; levels of active Vav-2 also appeared diminished in basal conditions (Fig. 8*B*). However, siRNA treatment had no effect on activated Src levels. In all, these results indicate that filamin B depletion significantly affects endothelial cell signaling, particularly at the cell adhesion and migration level, blocking Vav-2 stimulation by VEGF and altering normal Rac-1 activation/inactivation.

DISCUSSION

In the present study, we show that disruption of filamin B function is associated with loss of the proangiogenic effect of VEGF in three-dimensional collagen gels and inhibition of cell migration. We propose a key role for filamin B as a scaffolding protein coupling Rac-1 to Vav-2 and other extra- and intracellular signaling molecules.

Our results confirm high levels of filamin B expression in HUVEC and other endothelial cell types, such as 1G11 and

H5V. In addition, we compared filamin A and B expression in vessels from adult mouse tissues. We readily detected filamin A expression in vessels, but it was present in smooth muscle cells as well as in endothelial cells; in contrast, filamin B was almost specific to endothelial cells. Co-expression of different types of filamins in the same cell has been described for other cell types (16, 19, 40–42); however, these isoforms appear to play different functions in endothelial cells. Our results indicate a key role for filamin B in VEGF-stimulated angiogenesis *in vitro* in collagen gels, more specifically in the regulation of endothelial cell motility. Thus, knockdown of filamin B caused a profound effect on both endothelial cell migration and formation of tubular structures. In contrast, ablation of filamin A expression by siRNA treatment led only to a slight decrease in the capacity of endothelial cells to migrate. This differential role of filamins in the endothelium could explain the different vascular phenotypes observed in filamin A- and B-deficient mice. Thus, vessels from filamin A-deficient embryos are present but are disorganized, coarse, and exuberant (20). Endothelial cells from these animals present normal architecture and distribution of F-actin, normal filopodia, and membrane protrusions but low levels of VE-cadherin and abnormal adherent junctions (20). All of these results indicate that knockdown of filamin A causes an alteration in endothelium organization rather than a more specific decrease in endothelial cell migration. In contrast, defects described in microvasculature of filamin B-deficient mice may be the result of altered endothelial cell migration (23).

Cell migration implicates coordination in space and time of cytoskeletal changes that affect the formation of protrusions and adhesions at the migration front but also that elicit retraction of the old adhesions at the rear of the cell (43). The Rho family of GTPases plays a key role in the regulation of

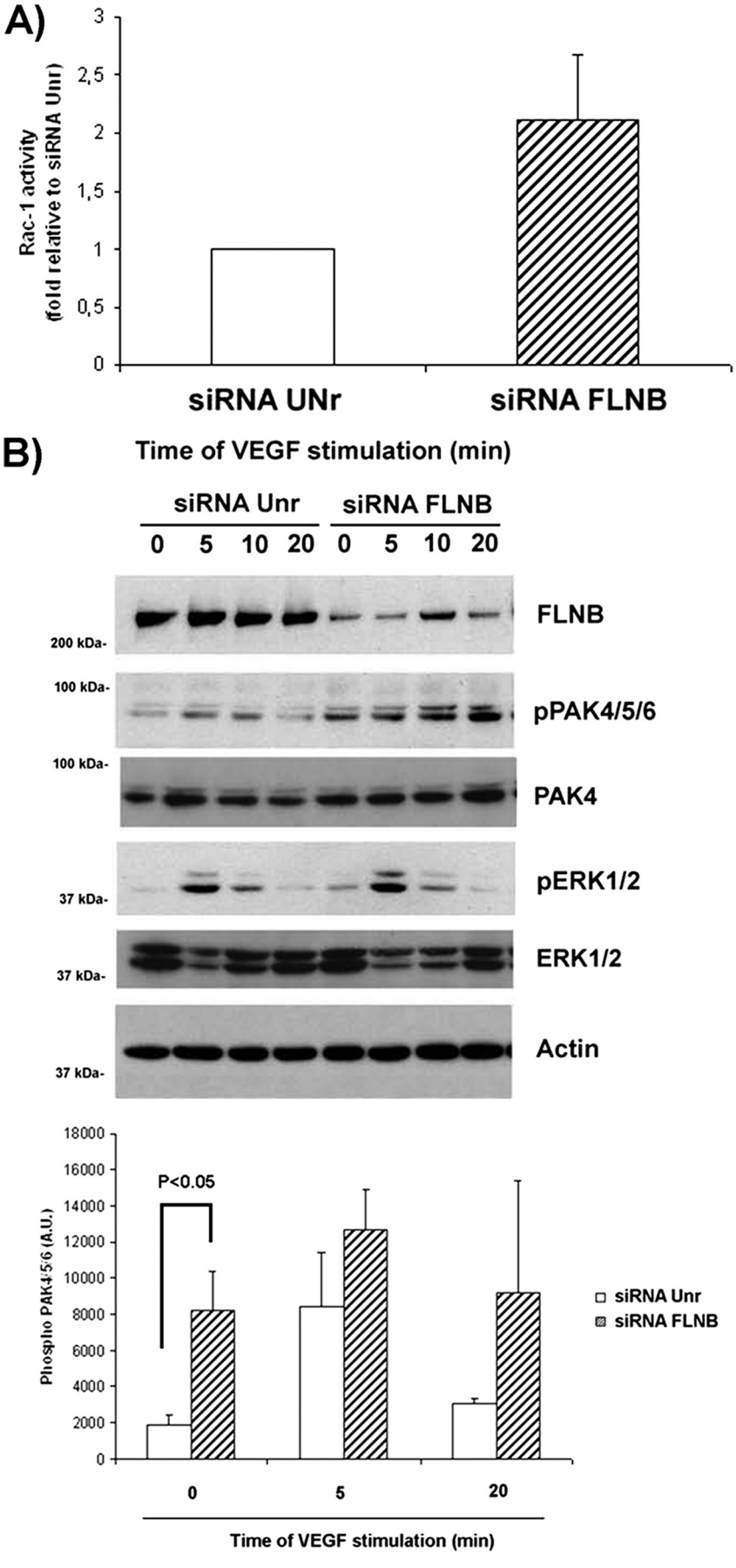

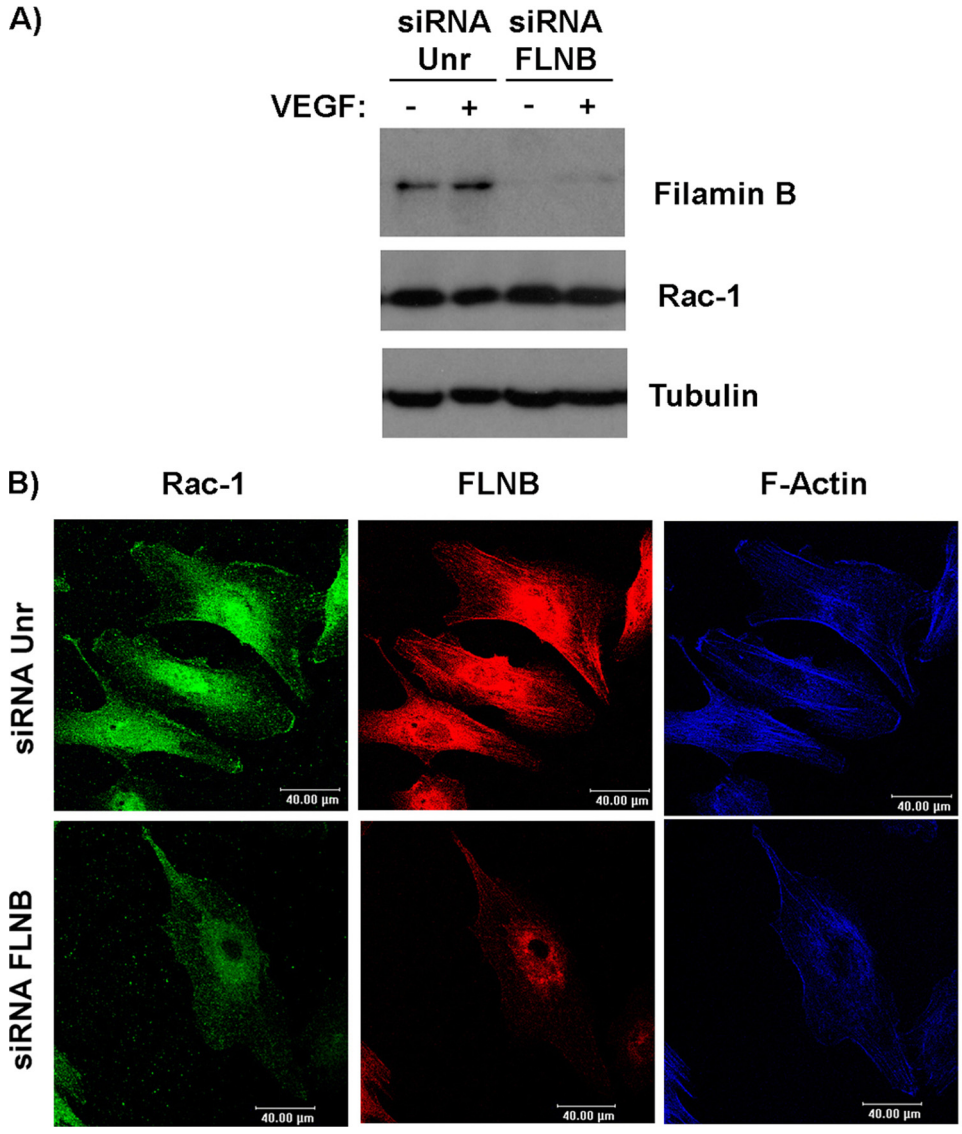

FIGURE 6. **Filamin B depletion blocks Rac-1 VEGF-induced translocation to plasma membrane.** *A*, HUVEC were transiently transfected with an unrelated control siRNA (*Unr*) or siRNA-FLNB3 as described, in the absence or presence of 20 ng/ml VEGF for 30 min. Cells were lysed, and FLNB, Rac-1, and tubulin (as a loading control) were immunodetected by Western blotting. A representative blot of three different experiments is shown. *B*, immunolocalization of F-actin (*blue*), Rac-1 (*green*), and filamin B (*red*) in HUVEC transiently transfected with an unrelated control siRNA or siRNA-FLNB3, as described, in the presence of 20 ng/ml VEGF for 30 min. *Bar*, 40 μm.

migration-related processes, with Rac and Cdc42 driving formation of the migration front and Rho controlling contraction at the rear (36, 43). Filamins participate in responses to extracellular signals that affect the cytoskeleton and cause changes in motility (12–14, 44). Our experiments showed that endothelial cells with low levels of filamin B present a flattened phenotype with increased adhesion to extracellular matrix (focal adhesions and contacts) in the basal state. After stimulation with VEGF, cells extended protrusions, polymerized actin, and generated stress fibers but lacked a well defined migration front. Altogether, these cells appeared to be defective in the stabilization of new adhesions by interaction with the extracellular matrix or in detachment of the old adhesions. These defects could be explained by an alteration of Vav-2-Rac-1-PAK signaling. In endothelial cells, PAK activity is necessary for migration, and it is up-regulated by the formation of new adhesions; in accordance with this, overexpression of a PAK dominant negative form inhibits cell migration (45). However, transfection of a constitutively active PAK mutant was also detrimental for migration because PAK inactivation is required for detachment and tail retraction. Taken together, these results indicate that a delicate balance in the activity of PAK is necessary during cell migration (45). In our filamin B depletion experiments, we observe a decrease in cell migration associated with an increase of focal adhesions; these changes are accompanied by deregulation of Rac-1-PAK activities, which appear increased even in basal conditions. Moreover, we have shown that alteration of Rac-1 normal activity in endothelial cells by overexpression of constitutively active or dominant negative Rac-1 isoforms affects the endothelial phenotype and also the ability of endothelial cells to migrate and organize in collagen gels. Therefore, it can be speculated that filamin B depletion causes a disruption of Rac-1-PAK signaling that results in PAK deregulation and defects in endothelial cell migration. We also show that expression of filamin B is essential for translocation of Rac-1 to the plasma membrane

FIGURE 5. **Filamin B depletion causes overstimulation of Rac-1 and PAK-4/5/6 basal activities in the absence of any effect on ERK1/2.** *A*, Rac-1 activity was measured using a G-LISA assay. Unrelated siRNA (*UNr*)- or siRNA-FLNB3-transfected cell lysates were incubated with an active Rac-binding protein bound to the bottom of a 96-well plate. After extensive washing, bound active Rac was detected with an anti-Rac antibody, followed by incubation with a secondary antibody conjugated with horseradish peroxidase. Detection reagent was added, and absorbance was measured at 595 nm. Results are expressed as relative to unrelated siRNA-transfected cells and represent an average of three experiments ± S.E. *B*, HUVEC were transiently transfected with the different siRNAs as described earlier. After 24 h of transfection, cells were depleted of growth factors for 16 h and stimulated with 20 ng/ml VEGF for the indicated periods of time. Cells were lysed, and FLNB, phospho-PAK-4/5/6 (*pPAK-4/5/6*), total PAK4, phospho-ERK1/2 (*pERK*), total ERK1/2, and β-actin (as a loading control) were immunodetected by Western blotting. A representative blot of five different experiments is shown. Densitometric quantification relative to loading control and mean ± S.E. of the five experiments is shown. Phospho-PAK-4/5/6 was significantly increased by filamin B depletion ($p < 0.05$ *t* test).

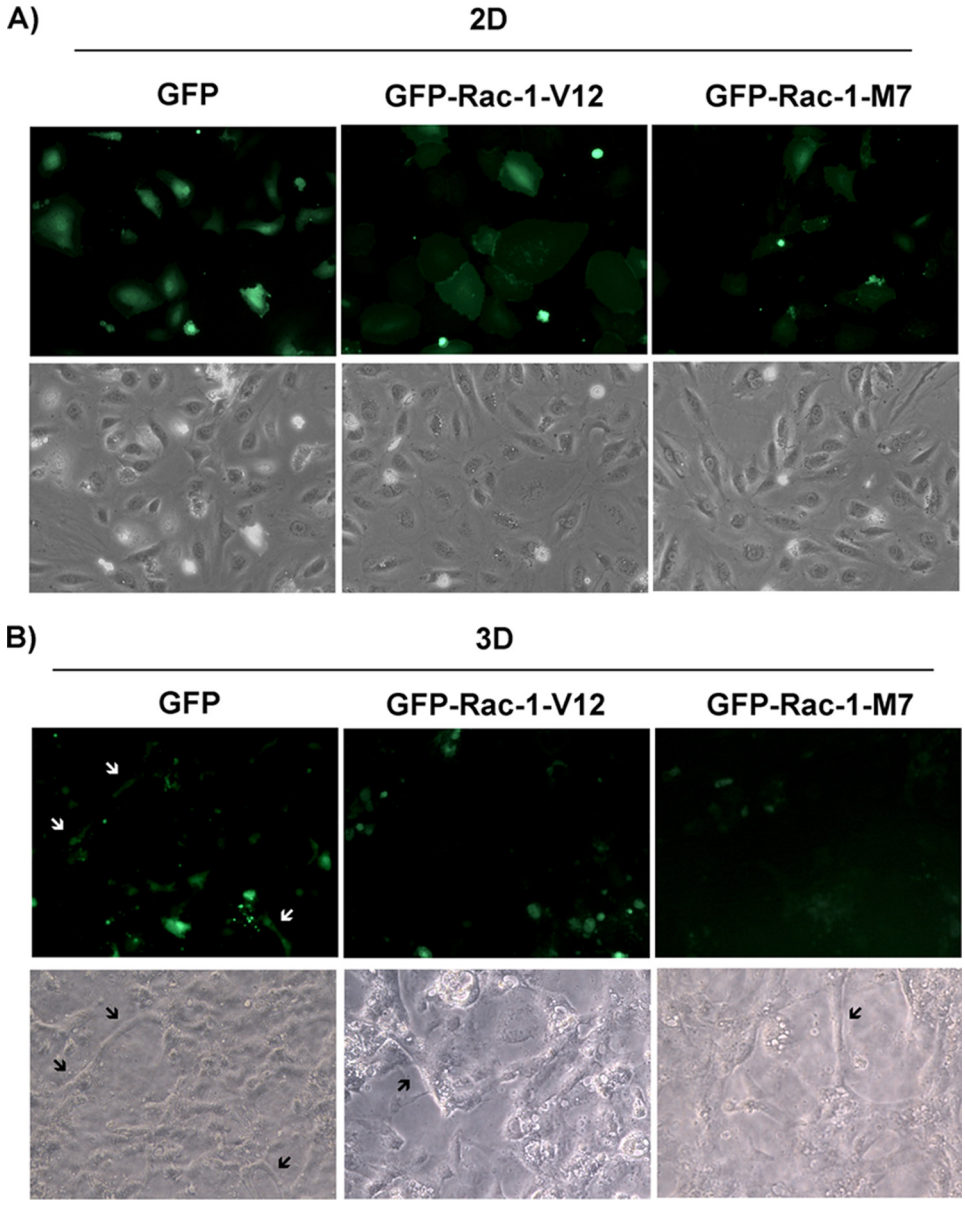

FIGURE 7. **Alteration of Rac-1 activity affects HUVEC phenotype and ability to form tubular structures.** *A*, HUVEC cultured in two-dimensional (*2D*) plates were transiently transfected with GFP, GFP-Rac1-V12 (a constitutively active form of Rac-1), or GFP-Rac1-M7 (a dominant negative form of Rac-1) as described. After 24 h, phase-contrast and fluorescent images of each experiment were captured on a Leica inverted phase-contrast microscope (×20). Overexpression of GFP-Rac1-V12 resulted in a flat phenotype, whereas GFP-Rac1-M7 caused a mixed effect, with some cells presenting a flat phenotype and others showing a normal shape. *B*, after 24 h, HUVEC transfected as in *A* were trypsinized and immersed in collagen gels (three-dimensional cultures (*3D*)) in the presence of 40 ng/ml VEGF for an additional 24 h. Phase-contrast and fluorescent images of each experiment were captured on a Leica inverted phase-contrast microscope (×20). Cells transfected with GFP were readily incorporated into pseudotubular structures formed in collagen gels (*arrows*), whereas cells with deregulated Rac-1 activity were excluded from these structures.

after VEGF stimulation, an essential step for cell migration (36–38). Thus, filamin B plays a key role in the control of Rac-1-PAK signaling necessary for the cycles of attachment and detachment that take place during cell migration. Our results suggest that filamin B exerts this role by acting as a scaffolding protein, facilitating the interaction of Rac-1 and the guanine nucleotide exchange factor Vav-2, which controls Rac-1 stimulation in endothelial cells (39). Filamin B is bound to Vav-2 and Rac-1 in basal conditions, ensuring the proper interaction of these proteins with VEGFR2 and proangiogenic integrins after VEGF stimulation and their subsequent activation. In the absence of filamin B, this signaling cascade is altered; VEGFR2 can still stimulate Src and ERK, but Vav-2 phosphorylation is inhibited. In these conditions, Rac-1 is deregulated, and its activity increases. The mechanism behind this increase in Rac-1 activity in filamin B-depleted cells will require further investigation. We can speculate that alteration of Rac-1 intracellular location could affect its normal cycles of activation/inactivation necessary for normal endothelial cell migration. An alternative scenario is that filamin B could facilitate the interaction of Rac-1 not only with the activator Vav-2 but also with a GTPase-activating protein (GAP) and thus mediate its inactivation. A candidate GAP for this role was FilGAP, a Rho-regulated GTPase-activating protein that inactivates Rac-1, promoting cell retraction through its interaction with filamin A (46). We failed to detect interaction between FilGAP and filamin B by immunoprecipitation experiments (data not shown), but the possibility remains that filamin B interacts with another GAP that might modulate Rac-1 activity.

Our results suggest that the effects exerted by filamin B on endothelial cells are mediated by its capacity to form signaling complexes, including FLNB, Rac-1, Vav-2, VEGFR2, and integrin $\alpha v\beta 5$, following VEGF stimulation. A similar scaffolding role has been described for filamin A; this protein has been shown to interact with prostate-specific membrane antigen and stimulate Rac-1 activity and endothelial cell migration through regulation of its interaction with integrins (47). Furthermore, as described before, filamin A mediates the interaction between Rac-1 and FilGAP (46). An article from Jeon *et al.* (41) has already described an interaction between Rac-1 and filamin B, proposing a role for filamin B as a scaffold protein in type I interferon signaling, linking Rac-1 and the JNK cascade module in HeLa cells. Our results confirm this interaction and describe a new function for filamin B in the endothelial cell context, not only in maintaining cellular structure but

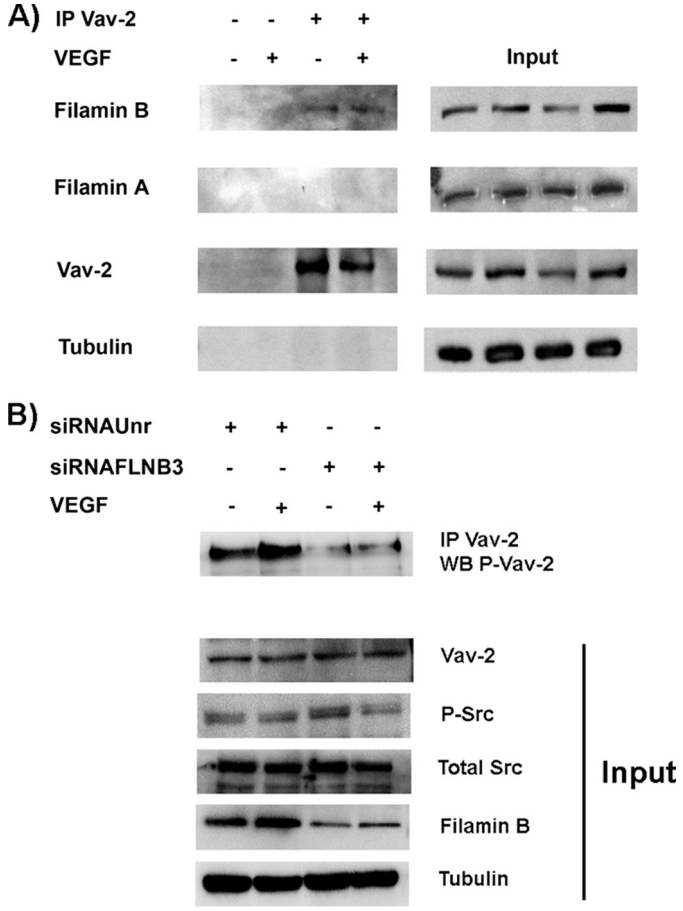

FIGURE 8. **Filamin B binds Vav-2 in basal conditions and after VEGF stimulation, and its depletion abolishes Vav-2 phosphorylation in the absence of any effect of Src phosphorylation.** *A*, HUVEC were starved for 16 h and then stimulated or not with 10 ng/ml VEGF for 30 min. Cell lysates were immunoprecipitated (*IP*) with or without anti-Vav-2 antibody, and filamin B was detected by Western blotting as described before. As a loading control, Western blotting with total lysates before immunoprecipitation was also performed. A representative blot of three different experiments is shown. *B*, HUVEC transiently transfected with an unrelated control siRNA (*Unr*) or siRNA-FLNB3 were depleted of growth factors for 16 h and stimulated or not with 10 ng/ml VEGF for 30 min. Cells were lysed and immunoprecipitated with anti-Vav-2 antibody. Phospho-Vav-2 was then detected by Western blotting in the immunoprecipitated samples. Total lysates were also analyzed as a loading control.

also in facilitating cell migration following VEGF stimulation, an essential process for angiogenesis.

Acknowledgments—We thank Jacques Pouysségur (Institute of Cellular Signaling, Developmental Biology, and Cancer Research, CNRS, Nice, France), Cristina Gamell and Gustavo Egea (Universitat de Barcelona), Mireia Duñach and Jesus Ruberte (Universitat Autònoma de Barcelona), Alan Hall (Memorial Sloan-Kettering Cancer Center, New York), and David García Molleví (Institut Català d'Oncologia-IDIBELL) for reagents and technical support; Francesc Mitjans (Merck Farma y Química, Barcelona, Spain) for integrin antibodies; and Esther Castaño and Benjamín Torrejón (Serveis Cientificotècnics de la Universitat de Barcelona), Ester Adanero and Aurea Navarro (Universitat de Barcelona), and Maria Molas (Universitat Autònoma de Barcelona) for technical support.

REFERENCES

1. Folkman, J., and Shing, Y. (1992) *J. Biol. Chem.* **267,** 10931–10934
2. Hanahan, D., and Folkman, J. (1996) *Cell* **86,** 353–364
3. Carmeliet, P. (2003) *Nat. Med.* **9,** 653–660
4. Jain, R. K. (2003) *Nat. Med.* **9,** 685–693
5. Dejana, E. (2004) *Nat. Rev. Mol. Cell Biol.* **5,** 261–270
6. Revenu, C., Athman, R., Robine, S., and Louvard, D. (2004) *Nat. Rev. Mol. Cell Biol.* **5,** 635–646
7. Critchley, D. R. (2000) *Curr. Opin. Cell Biol.* **12,** 133–139
8. Calderwood, D. A., Shattil, S. J., and Ginsberg, M. H. (2000) *J. Biol. Chem.* **275,** 22607–22610
9. Rousseau, S., Houle, F., Landry, J., and Huot, J. (1997) *Oncogene* **15,** 2169–2177
10. Rousseau, S., Houle, F., Kotanides, H., Witte, L., Waltenberger, J., Landry, J., and Huot, J. (2000) *J. Biol. Chem.* **275,** 10661–10672
11. Lee, J. S., and Gotlieb, A. I. (2003) *Histol. Histopathol.* **18,** 879–887
12. van der Flier, A., and Sonnenberg, A. (2001) *Biochim. Biophys. Acta* **1538,** 99–117
13. Stossel, T. P., Condeelis, J., Cooley, L., Hartwig, J. H., Noegel, A., Schleicher, M., and Shapiro, S. S. (2001) *Nat. Rev. Mol. Cell Biol.* **2,** 138–145
14. Popowicz, G. M., Schleicher, M., Noegel, A. A., and Holak, T. A. (2006) *Trends Biochem. Sci.* **31,** 411–419
15. Zhang, W., Han, S. W., McKeel, D. W., Goate, A., and Wu, J. Y. (1998) *J. Neurosci.* **18,** 914–922
16. Sheen, V. L., Feng, Y., Graham, D., Takafuta, T., Shapiro, S. S., and Walsh, C. A. (2002) *Hum. Mol. Genet.* **11,** 2845–2854
17. Takafuta, T., Wu, G., Murphy, G. F., and Shapiro, S. S. (1998) *J. Biol. Chem.* **273,** 17531–17538
18. Wang, Q., Patton, W. F., Hechtman, H. B., and Shepro, D. (1997) *J. Cell. Physiol.* **172,** 171–182
19. Kanters, E., van Rijssel, J., Hensbergen, P. J., Hondius, D., Mul, F. P., Deelder, A. M., Sonnenberg, A., van Buul, J. D., and Hordijk, P. L. (2008) *J. Biol. Chem.* **283,** 31830–31839
20. Feng, Y., Chen, M. H., Moskowitz, I. P., Mendonza, A. M., Vidali, L., Nakamura, F., Kwiatkowski, D. J., and Walsh, C. A. (2006) *Proc. Natl. Acad. Sci. U.S.A.* **103,** 19836–19841
21. Hart, A. W., Morgan, J. E., Schneider, J., West, K., McKie, L., Bhattacharya, S., Jackson, I. J., and Cross, S. H. (2006) *Hum. Mol. Genet.* **15,** 2457–2467
22. Lu, J., Lian, G., Lenkinski, R., De Grand, A., Vaid, R. R., Bryce, T., Stasenko, M., Boskey, A., Walsh, C., and Sheen, V. (2007) *Hum. Mol. Genet.* **16,** 1661–1675
23. Zhou, X., Tian, F., Sandzén, J., Cao, R., Flaberg, E., Szekely, L., Cao, Y., Ohlsson, C., Bergo, M. O., Borén, J., and Akyürek, L. M. (2007) *Proc. Natl. Acad. Sci. U.S.A.* **104,** 3919–3924
24. Farrington-Rock, C., Kirilova, V., Dillard-Telm, L., Borowsky, A. D., Chalk, S., Rock, M. J., Cohn, D. H., and Krakow, D. (2008) *Hum. Mol. Genet.* **17,** 631–641
25. Dong, Q. G., Bernasconi, S., Lostaglio, S., De Calmanovici, R. W., Martin-Padura, I., Breviario, F., Garlanda, C., Ramponi, S., Mantovani, A., and Vecchi, A. (1997) *Arterioscler. Thromb. Vasc. Biol.* **17,** 1599–1604
26. Viñals, F., López-Rovira, T., Rosa, J. L., and Ventura, F. (2002) *FEBS Lett.* **510,** 99–104
27. McKenzie, F. R., and Pouysségur, J. (1996) *J. Biol. Chem.* **271,** 13476–13483
28. Laemmli, U. K. (1970) *Nature* **227,** 680–685
29. Garlanda, C., Parravicini, C., Sironi, M., De Rossi, M., Wainstok de Calmanovici, R., Carozzi, F., Bussolino, F., Colotta, F., Mantovani, A., and Vecchi, A. (1994) *Proc. Natl. Acad. Sci. U.S.A.* **91,** 7291–7295
30. Abedi, H., and Zachary, I. (1997) *J. Biol. Chem.* **272,** 15442–15451
31. Soga, N., Namba, N., McAllister, S., Cornelius, L., Teitelbaum, S. L., Dowdy, S. F., Kawamura, J., and Hruska, K. A. (2001) *Exp. Cell Res.* **269,** 73–87
32. Gong, C., Stoletov, K. V., and Terman, B. I. (2004) *Angiogenesis* **7,** 313–321
33. Kobayashi, M., Nishita, M., Mishima, T., Ohashi, K., and Mizuno, K. (2006) *EMBO J.* **25,** 713–726
34. Eliceiri, B. P., Puente, X. S., Hood, J. D., Stupack, D. G., Schlaepfer, D. D.,

Huang, X. Z., Sheppard, D., and Cheresh, D. A. (2002) *J. Cell Biol.* **157,** 149–160
35. Eliceiri, B. P., Paul, R., Schwartzberg, P. L., Hood, J. D., Leng, J., and Cheresh, D. A. (1999) *Mol. Cell* **4,** 915–924
36. Etienne-Manneville, S., and Hall, A. (2002) *Nature* **420,** 629–635
37. Del Pozo, M. A., Kiosses, W. B., Alderson, N. B., Meller, N., Hahn, K. M., and Schwartz, M. A. (2002) *Nat. Cell Biol.* **4,** 232–239
38. ten Klooster, J. P., Jaffer, Z. M., Chernoff, J., and Hordijk, P. L. (2006) *J. Cell Biol.* **172,** 759–769
39. Garrett, T. A., Van Buul, J. D., and Burridge, K. (2007) *Exp. Cell Res.* **313,** 3285–3297
40. Krakow, D., Robertson, S. P., King, L. M., Morgan, T., Sebald, E. T., Bertolotto, C., Wachsmann-Hogiu, S., Acuna, D., Shapiro, S. S., Takafuta, T., Aftimos, S., Kim, C. A., Firth, H., Steiner, C. E., Cormier-Daire, V., Superti-Furga, A., Bonafe, L., Graham, J. M., Jr., Grix, A., Bacino, C. A., Allanson, J., Bialer, M. G., Lachman, R. S., Rimoin, D. L., and Cohn, D. H. (2004) *Nat. Genet.* **36,** 405–410
41. Jeon, Y. J., Choi, J. S., Lee, J. Y., Yu, K. R., Ka, S. H., Cho, Y., Choi, E. J., Baek, S. H., Seol, J. H., Park, D., Bang, O. S., and Chung, C. H. (2008) *Mol. Biol. Cell* **19,** 5116–5130
42. van der Flier, A., Kuikman, I., Kramer, D., Geerts, D., Kreft, M., Takafuta, T., Shapiro, S. S., and Sonnenberg, A. (2002) *J. Cell Biol.* **156,** 361–376
43. Ridley, A. J., Schwartz, M. A., Burridge, K., Firtel, R. A., Ginsberg, M. H., Borisy, G., Parsons, J. T., and Horwitz, A. R. (2003) *Science* **302,** 1704–1709
44. Feng, Y., and Walsh, C. A. (2004) *Nat. Cell Biol.* **6,** 1034–1038
45. Kiosses, W. B., Daniels, R. H., Otey, C., Bokoch, G. M., and Schwartz, M. A. (1999) *J. Cell Biol.* **147,** 831–844
46. Ohta, Y., Hartwig, J. H., and Stossel, T. P. (2006) *Nat. Cell Biol.* **8,** 803–814
47. Conway, R. E., Petrovic, N., Li, Z., Heston, W., Wu, D., and Shapiro, L. H. (2006) *Mol. Cell. Biol.* **26,** 5310–5324